Letter

Simultaneous memory effects in the stress and in the dielectric susceptibility of a stretched polymer glass

J. Hem,[1] C. Crauste-Thibierge ●,[1] F. Clément,[2] D. R. Long ●,[2] and S. Ciliberto[1]

[1]*Univ of Lyon, Ens de Lyon, Univ Claude Bernard, CNRS, Laboratoire de Physique, UMR 5672, F-69342 Lyon, France*
[2]*Laboratoire Polymères et Matériaux Avancés, CNRS/Solvay, UMR 5268, 69192 Saint Fons Cedex, France*

We report experimental evidence that a polymer stretched at constant strain rate $\dot{\lambda}$ presents complex memory effects after $\dot{\lambda}$ is set to zero at a specific strain λ_w for a duration t_w, ranging from 100 s to 2.2×10^5 s. When the strain rate is resumed, both the stress and the dielectric constant relax to the unperturbed state nonmonotonically. The relaxations depend on the observable, on λ_w and on t_w. Relaxation master curves are obtained by scaling the time and the amplitudes by $\ln(t_w)$. The dielectric evolution also captures the distribution of the relaxation times, so the results impose strong constraints on the relaxation models of polymers under stress and they can be useful for a better understanding of memory effects in other disorder materials.

Aging of amorphous and heterogeneous materials is characterized by a slow relaxation toward a new state after a perturbation has been applied [1]. This relaxation usually spans several orders of magnitude in time and may present memory effects, which depend on the sample history (see Ref. [2] for a recent review).

Memory effects have been observed in glassy and disordered materials [3–18], and also in many other disordered systems [19–26]. Memory effects may take the form of a Kovacs-like nonmonotonic relaxation, in which the response of a state variable, to an external perturbation, evolves in one direction before turning around at a timescale and an amplitude which depend on the sample history. These Kovacs-like relaxations have been observed in the mechanical [6–12] and electrical [13] responses of polymer glasses and melts [18], in the static coefficient of friction [19,20], in the load on crumpled thin sheets [21,22], and in the mechanical response of granular systems [23–26].

Several theoretical models [27–32] have been developed to explain, with common underlying physical principles, the similar features of these complex relaxations observed in very different systems. One of the key assumptions of these models is the existence in these disordered systems of a distribution of relaxation times (DRT) which is used to explain the origin of aging and of nonmonotonic relaxations. However, it is hard to discern between the different descriptions using experiments in which only one observable is measured. Thus to give more insight into this problem, we performed experiments on a stretched polymer glass where one gets quantitative information on the memory of several observables measured simultaneously and on the evolution of the DRT.

In this Letter we describe these experiments and report the observation that a stretched polymer glass exhibits complex memory effects of both the stress and of the dielectric susceptibility. Specifically, we show that, after a perturbation of the strain rate, the relaxation dynamics of the stress and the dielectric susceptibility present nonmonotonic responses which depend not only on the sample history, as in the above-mentioned Kovacs-like memory effect, but also on the observable. Furthermore, from the evolution of the dielectric spectra, we get insights on the evolution of the polymer DRT. Thus our results impose constraints for modeling not only the universal features of memory effects but also the polymer relaxation dynamics under deformation, which is widely studied, both experimentally [33–40] and theoretically [27,41–45].

In our experiment the investigated polymer is an extruded film MAKROFOL DE® 1-1 000000 from BAYER based on Makrolon® polycarbonate (PC) of thickness 125 μm. The films are cut into rectangular pieces of size 42×21 cm with a dog bone shape before being tied to the tensile machine. During the experiment, we measure the instantaneous stress $\sigma(t)$ and deformation $\lambda(t) = L(t)/L_0$ of the films. The experiments are performed at imposed $\dot{\lambda} \simeq 10^{-4}$ s and at $T = 25\,^\circ$C much below the glass transition temperature $T_g = 150\,^\circ$C. In parallel to the stress measurement we use the dielectric spectroscopy to investigate the dynamics of the relaxation processes at work in the stretched PC film [46,47]. Dielectric spectroscopy is indeed a convenient way to probe *in situ* and without destruction the relaxation times of stretched polymers [38–40]. It is worth mention that other techniques, such as NMR measurements [33] or probe molecule experiments [34,35], can be used but dielectric spectroscopy is very versatile. In the rest of the Letter, we will focus only on the loss tangent $\tan\delta(f) = -\epsilon''(f)/\epsilon'(f)$, which does not depend on the film thickness, being the ratio of the imaginary (ϵ'') and real (ϵ') parts of the dielectric susceptibility, at frequency f. For the dielectric measure of our samples, the film is sandwiched between two electrodes and conductive gel layers which ensure a uniform electrical contact. The electrodes are connected to a home-made dielectric spectrometer, which measures the dielectric spectrum every 32 s in the frequency range $[10^{-1}–10^3]$ Hz,
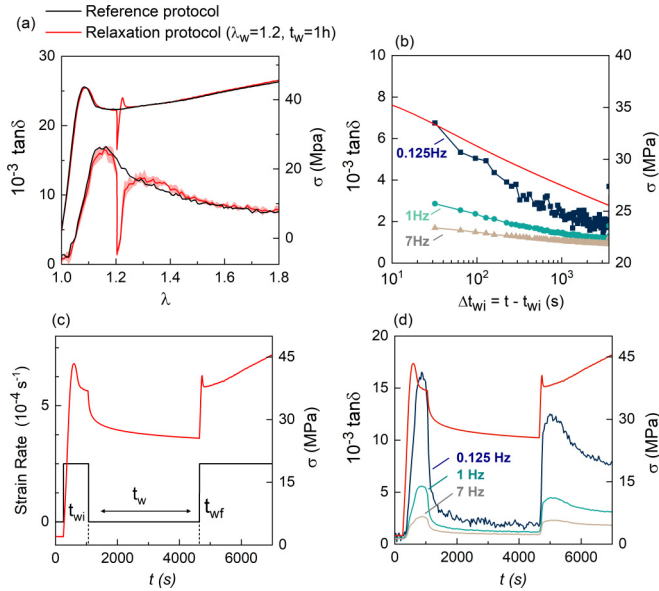
FIG. 1. (a) Dielectric susceptibility $\tan\delta$ at $f = 0.125$ Hz and nominal stress $\sigma = F/S_o$ with $S_o = 210\times0.125$ mm^2 as a function of the strain λ. Black lines: constant strain rate protocol $\dot{\lambda} = 2.5\times10^{-4}$ s^{-1}, called reference curves. Red lines: relaxation protocol $\lambda_w = 1.2$ and $t_w = 1$ h. The red line thickness corresponds to one standard deviation. (b) Temporal evolution $\tan\delta$ at $f = 0.125, 1, 7$ Hz and σ during the waiting step over $t_w = 1$ h. (c) $\dot{\lambda}(t)$ and $\sigma(t)$ during the relaxation protocol with $\lambda_w = 1.2$, $t_w = t_{wf} - t_{wi} = 1$ h. Times t_{wi} and t_{wf} delimit the beginning and the end of the waiting interval, respectively. (d) $\tan\delta(t)$ at $f = 0.125, 1, 7$ Hz and $\sigma(t)$.

simultaneously on all of the frequencies and with an accuracy of a few percent [48]. Thus it allows us to follow the evolution of the dielectric spectra during the stretching protocols which lasts more than 2 h. In order to get the required repeatability, we average the results over at least three tests performed in different samples submitted to the same stretching protocol. More details about the experimental apparatus can be found in Refs. [38,39,48].

We first recall the behavior of the stress and the dielectric susceptibility as a function of λ measured at constant strain rate $\dot{\lambda}$, that we have discussed in Refs. [38,39]. Figure 1(a) depicts the stress evolution for polycarbonate at $\dot{\lambda} = 2.5 \times 10^{-4}$ s^{-1} (black curve). The stress first increases until the yield stress at about $\lambda = 1.08$, then, successively decreases,—a regime known as strain softening—reaches a plateau at about $\lambda = 1.20$, and finally increases again, which is known as strain hardening. The breaking occurs at about $\lambda = 1.8$–2 [49]. The dielectric spectra in the range $[10^{-1}$–$10^3]$ Hz have been measured every 32 s, during which λ has a negligible increase of less than 0.8% at this $\dot{\lambda}$. As described in Refs. [38–40], dielectric measurements give access to the evolution of the dominant relaxation time τ_α of the polymer [50] by identifying the lower part of the dielectric spectrum as the high frequency tail of the α relaxation peak. In particular, we have shown in Ref. [39] that the increase (decrease) of the dielectric susceptibility in the range $[10^{-1}$–$10^3]$ Hz reflects a decrease (increase) of τ_α, which depends on λ and the strain rate $\dot{\lambda}$. Therefore, the evolution of $\tan\delta$ at $f = 0.125$ Hz depicted in Fig. 1(a) shows

an acceleration of the relaxation times until the softening or onset of plastic flow (maximum around $\lambda = 1.15$–1.17) and a slowdown during the strain hardening regime that we have studied in Ref. [39]. The results of the measurements performed at constant $\dot{\lambda}$ [black curves in Fig. 1(a)] will be called "reference curves".

To investigate the memory effect, we have modified the protocol at constant $\dot{\lambda}$ in order to include an aging step at a specific λ in the post yield regime of the film. More precisely, the film is first stretched at $\dot{\lambda} = 2.5\times10^{-4}$ s^{-1}, then held at the waiting strain λ_w during the waiting time t_w, and finally further stretched with the same initial $\dot{\lambda}$. As an example for the case $\lambda_w = 1.2$ (plastic flow) and $t_w = 1$ h, the evolutions of σ and of $\tan\delta(0.125)$ are illustrated as a function of λ in Fig. 1(a). The corresponding time evolution is illustrated in Figs. 1(c) and 1(d) where the instantaneous strain rate $\dot{\lambda}$ is indicated, too. Three different intervals can be distinguished: During the initial one ($\lambda < \lambda_w$ and $t < t_{wi}$), σ and $\tan\delta$ are identical to the reference curves [see Fig. 1(a)]. During the waiting interval (i.e., $\lambda_w = 1.2$ and $t_{wi} \leqslant t \leqslant t_{wf}$), they decrease logarithmically with time, which is the signature of an aging process [see Fig. 1(b)]. Finally as soon as $\dot{\lambda}$ is resumed for $t \geqslant t_{wf}$, they increase again. In Fig. 1(a), the comparison with the reference curves obtained with the constant $\dot{\lambda}$ protocol shows that σ and $\tan\delta(0.125)$ finally recover their reference curves. However, notice that, in spite of the fact that σ and $\tan\delta(0.125)$ have a similar dependence on λ before the aging step, the recoveries of the two observables are rather different [see Fig. 1(a)]. In addition, we shall see that these recovery processes also depend on t_w and on λ_w.

Before presenting these results, we point out that Fig. 1(d) shows that the response of $\tan\delta$ to λ increases by reducing the frequency f. From this frequency dependence we get useful information on the DRT evolution by studying the whole spectrum of $\tan\delta$. Thus we plot the $\tan\delta$ spectra in Fig. 2(a) during the waiting interval at $\lambda_w = 1.2$ and in Fig. 2(b) during the recovery for $t > t_{wf}$. We first notice that the spectra evolve in a significant way only for $f < 100$ Hz. Furthermore, we see in Fig. 2(a) that the spectrum at $\lambda = 1.2$, at the beginning of the aging ($t = t_{wi}$), is identical to the reference one obtained during the constant $\dot{\lambda}$ protocol. Then, during the waiting interval for increasing $\Delta t_{wi} = t - t_{wi}$, the spectrum progressively decreases towards the equilibrium spectrum (i.e., the spectrum at $\lambda = 1$). Inversely, in Fig. 2(b), the spectra during the recovery interval increase again until they reach the reference spectrum around $\lambda = 1.3$, i.e., $\Delta t = t - t_{wf} = 400$ s.

The main relaxation time can be estimated from these dielectric spectra following the method presented in Ref. [39] in which we have shown that at low frequencies $\tan\delta(f) \simeq (\sin\beta\pi/2)/(2\pi f \tau_{\text{eff}})^\beta$ where the characteristic time τ_{eff} and the exponent β have to be determined. Within the Cole-Cole [51] model, τ_{eff} is proportional to the main relaxation time τ_α of the polymer [52] and the exponent β is related to the width of the distribution of the relaxation times, specifically the smallest is $\beta < 1$, the larger is the distribution [37,39]. Thus the fit of the low frequencies part of the spectra in Figs. 2(a), and 2(b) (recorded at different times) allows us to estimate the evolution of the DRT during the relaxation protocol. In particular, we see in Figs. 2(c) and 2(d) that, during the waiting interval, τ_{eff} (β) increases (decreases),
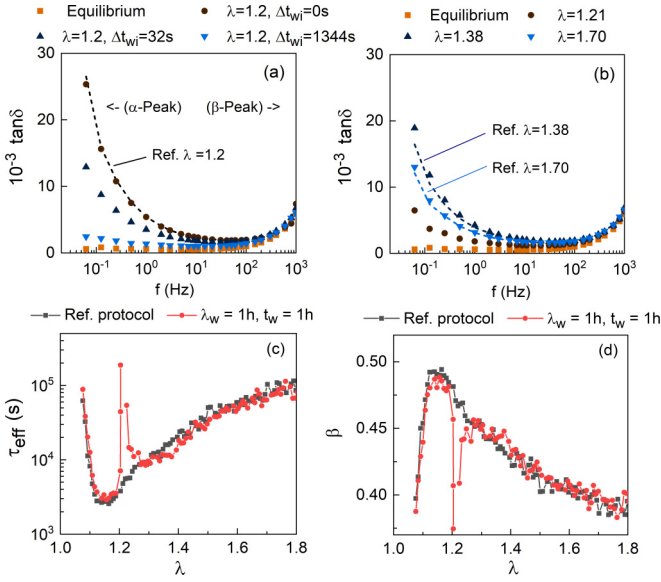
FIG. 2. Dielectric spectra tanδ recorded at different times for the relaxation protocol at $\lambda_w = 1.2$ and $t_w = 1$ h. (a) Evolution during the aging interval at $\lambda = 1.2$ with $\Delta t_{wi} = t - t_{wi}$ and (b) during the recovery interval for $\lambda > 1.2$. Dashed lines correspond to the reference spectra recorded at constant $\dot{\lambda}$. The evolutions of τ_{eff} and β are plotted in (c) and (d), respectively. Black line: constant $\dot{\lambda}$ protocol. Red line: relaxation protocol.
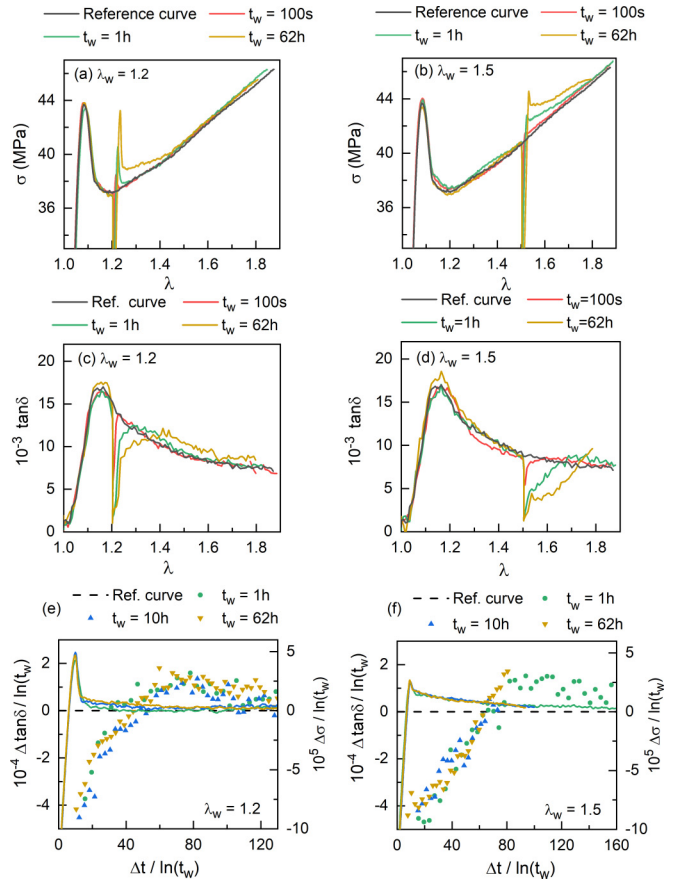

FIG. 3. (a)–(d) Stress σ and dielectric susceptibility tanδ at $f = 0.125$ Hz as a function of λ for different λ_w and t_w. Curves obtained by averaging three tests with $t_w = 62$ h and four tests with $t_w = 100$ s and 1 h. (a),(c) σ and tanδ at $\lambda_w = 1.2$ (in the plastic flow regime). (b),(d) σ and tanδ at $\lambda_w = 1.5$ (in the strain hardening). The reference curves are indicated in black. Note the stress axis has been expanded in (a) and (b) with respect to Fig. 1(a). (e),(f) Evolution of $\Delta\sigma / \ln(t_w)$ (continuous lines) and $\Delta\tan\delta / \ln(t_w)$ (symbols) as a function of $\Delta t / \ln(t_w)$ for $t \geqslant t_{wf}$, at (e) $\lambda_w = 1.2$ and (f) $\lambda_w = 1.5$ (see text for details).

meaning that not only the dynamics slow down but that the distribution of times is broadening. When the strain rate is resumed the dynamics accelerate again and the distribution shrinks, recovering the reference state after the resumption. Hence, this is the evidence that the DRT depends on the driving history and that $\dot{\lambda}$ accelerates the polymer dynamics, even if the acceleration is not monotonous in λ. The results of Fig. 2 strengthen quantitatively early observations on DRT reported in Ref. [36].

To study the evolution of tanδ as a function of t_w and λ_w, we now select tanδ measured at $f = 0.125$ Hz as a typical amplitude of the low frequency spectra, which depend on τ_α and β. Figures 3(a)–3(f) bring more details on the recovery processes by showing different results of tests performed with different waiting times and waiting strains $\lambda_w = 1.2$ (plastic flow) in Figs. 3(a) and 3(c) and $\lambda_w = 1.5$ (strain hardening) in Figs. 3(b) and 3(d). When $\dot{\lambda}$ is resumed at t_{wf}, we observe that the relaxations of σ and tanδ are both nonmonotonic and exhibit an overshoot above the reference curve before relaxing to it, with different shapes of the evolutions of the two observables. On one side, the stress overshoot has a distinct and large amplitude while occurring rapidly after the resumption [see Figs. 3(a) and 3(b)]. In contrast, the overshoot of tanδ has a weaker amplitude and occurs much later in time [see Figs. 3(c) and 3(d)].

Moreover, we find that the waiting time has a strong impact on the relaxation. In the case of σ, Figs. 3(a) and 3(b) show that, as long as t_w increases, the overshoot peak shifts progressively to longer time and presents a higher and sharper amplitude. In the case of tanδ, Figs. 3(c) and 3(d) show that an increase of t_w also shifts the peak time and slows down the

relaxation to the reference curve. Also in the dielectric case, we observe that a longer t_w affects the peak amplitude.

Besides the waiting time, the choice of the waiting strain also modifies the relaxation. Figures 3(a) and 3(b) show qualitatively that the stress overshoot peak is higher and narrower at $\lambda_w = 1.2$ than at $\lambda_w = 1.5$ and at the same time Figs. 3(c) and 3(d) show that tanδ recovers much faster the reference curve at $\lambda_w = 1.2$ than at $\lambda_w = 1.5$. The difference is significant. For example at $t_w = 1$ h and $\lambda_w = 1.2$, tanδ recovers the reference curve at about $\lambda = 1.45$, equivalent to $\Delta t = t - t_{wf} = 1024$ s after the resumption of the stretching. This is much faster than for the case at $t_w = 1$ h and $\lambda_w = 1.5$ for which the recovery is even too long to occur during our experiment ($\lambda > 1.85$ equivalent to $\Delta t > 1240$ s). In particular, this enhancement of the mobility recovery delay with λ_w fully supports the long one observed in multicreep experiments [36], in which the aging relaxation is performed in the strain hardening regime.

To be more precise regarding the dependence of the relaxations on those aging parameters, we analyze the difference

between the stress curve and the reference one $\Delta\sigma = \sigma - \sigma_{\text{ref}}$ as a function of the time $\Delta t = t - t_{wf}$ elapsed after resumption. Figures 3(e) and 3(f) show that all the relaxation curves, measured after different waiting times t_w, can be superimposed on a master curve by scaling $\Delta\sigma$ and Δt by $\ln(t_w)$, for $t_w > 100$ s. Moreover, we observe that this relation holds regardless of the waiting strain value ($\lambda_w = 1.2$ or $\lambda_w = 1.5$). As a consequence, this means that the peak time and the peak amplitude depend on $\ln(t_w)$. Regarding the dependence of the peak properties on t_w and λ_w, we note that the peak amplitude $\Delta\sigma_p$ is different for the two waiting strains, being higher at $\lambda_w = 1.2$ than at $\lambda_w = 1.5$ for all t_w. In contrast the peak time Δt_p is independent on the waiting strain [see Figs. 3(e) and 3(f)].

Finally, it is interesting to see that this way of scaling the data also works for the dielectric susceptibility. In a similar way as before, we have studied the evolution of the difference between the $\tan\delta$ curve at $f = 0.125$ Hz and the reference one $\Delta\tan\delta = \tan\delta - \tan\delta_{\text{ref}}$ as a function of Δt. Figures 3(e) and 3(f) show that all the relaxation curves merge on a master curve by rescaling $\Delta\tan\delta$ and Δt by $\ln(t_w)$. This is observed again for the two waiting strains investigated, either at $\lambda_w = 1.2$ [Fig. 3(c)] or at $\lambda_w = 1.5$ [Fig. 3(d)]. Note that for the dielectric case, the peak time at $\lambda_w = 1.5$ is delayed compared to $\lambda_w = 1.2$, which was not the case for the stress relaxation. The logarithmic dependence on t_w shows, in particular, that the memory of the aging history can also occur in $\tan\delta$, so that we provide evidence that the memory appears simultaneously in different observables but in different ways.

Concerning the scaling $\Delta t / \ln(t_w)$, we point out that in several systems with nonmonotonous relaxations, the memory effects present a $\Delta t/t_w$ scaling [2,22,30], which however is not generic. In several cases [4], a heuristic form of scaling $\Delta t/t_w^\mu$ is used, which has been theoretically justified [29]. If $\mu \ll 1$, then $\ln t_w$ cannot be distinguished from t_w^μ, and our scaling $\Delta t / \ln(t_w)$ can be understood within this theoretical framework. In these models the DRT does not depend on time, whereas our measurements show that it does evolve, thus our measure of the DRT evolution will help in constructing more precise models. It remains to understand why the timescale of the relaxations are different for σ and $\tan\delta$. It is interesting to notice that for polymers the amplitude of the main yield stress peak also undergoes a similar logarithmic dependence on the aging time $\tilde{t}_w$, which in this case is the time spent in the glassy state after a temperature quench from the melt [53–56]. However, in contrast to our experiment, the positions of the yield peak do not depend on $\tilde{t}_w$. This difference could be related to the way the waiting step is realized. Indeed, when the polymer ages after a temperature quench, no stress is applied to the sample before the measure of the loading curve, whereas in our experiment the polymer ages from the plastic regime at constant strain. From this perspective, it must be concluded that stretching substantially affects the aging and the recovery processes, which is confirmed by the dependence of the memory effects on λ observed in our experiment. The evolution of the dielectric susceptibility and of the DRT when a stress is applied after the time $\tilde{t}_w$ has never been measured, and no comparison with our results can be done. This comparison would be very useful for giving new insights into the polymer relaxations under stress.

In conclusion, we have shown that a stretched polymer presents complex memory effects in the nonmonotonous relaxations of σ and $\tan\delta$. Although nonmonotonous responses of σ have been already observed in stretched polymers [7–12] it is interesting to notice that $\tan\delta$ behaves in a similar way as a function of λ_w and t_w. Nonmonotonous relaxation of the dielectric susceptibility has been observed [13] after an electric field perturbation but never after a mechanical perturbation. This new observation is indeed very useful because the measure of $\tan\delta$ as a function of frequency allows us to have information on the evolution of the DRT during the stretching, the waiting, and the recovery intervals. The result of this measure strengthens previous observations on DRT [36] and brings new insight to the long-lasting debate on mechanical rejuvenation in polymers (see, e.g., [27,39]). The observed timescaling and DRT evolution is also useful when one tries to fit this observation into the more general models of memory effects which have been developed to explain the experimental observation in glassy and disordered systems. Thus our results, by showing important features of the dynamical processes of two interrelated quantities and of the polymer relaxation dynamics, challenge the theoretical models of the memory effect in glassy materials and disordered systems.

[1] L. C. E. Struik, *Physical Aging in Amorphous Polymers and Other Materials* (Elsevier, Oxford, 1978).

[2] N. C. Keim, J. D. Paulsen, Z. Zeravcic, S. Sastry, and S. R. Nagel, Rev. Mod. Phys. **91**, 035002 (2019).

[3] V. Dupuis, F. Bert, J. Bouchaud, J. Hamman, F. Ladieu, D. Parker, and E. Vincent, Pramana **64**, 1109 (2005).

[4] E. Vincent, in *Lecture Notes in Physics Vol. 716* (Springer-Verlag, Berlin, Heidelberg, 2007), pp. 7–60.

[5] H. E. Castillo, C. Chamon, L. F. Cugliandolo, and M. P. Kennett, Phys. Rev. Lett. **88**, 237201 (2002).

[6] A. J. Kovacs, Adv. Polym. Sci. **3**, 394 (1963).

[7] P. I. Vincent, Adv. Polym. Sci. **1**, 7 (1960).

[8] E. J. Kramer, J. Appl. Phys. **41**, 4327 (1970).

[9] T. Ricco and T. L. Smith, Polymer **26**, 1979 (1985).

[10] T. Ricco and T. L. Smith, J. Polym. Sci. Part B **28**, 513 (1990).

[11] A. F. Yee, R. J. Bankert, K. L. Ngai, and R. W. Rendell, J. Polym. Sci. Part B **26**, 2463 (1988).

[12] C. G'Sell and G. B. McKenna, Polymer **33**, 2103 (1992).

[13] A. Alegria, L. Goitiandia, I. Telleria, and J. Colmenero, Macromolecules **30**, 3881 (1997).

[14] L. Bellon, S. Ciliberto, and C. Laroche, Europhys. Lett. **51**, 551 (2000).

[15] L. Bellon, S. Ciliberto, and C. Laroche, Eur. Phys. J. B **25**, 223 (2002).

[16] A. Amir, S. Borini, Y. Oreg, and Y. Imry, Phys. Rev. Lett. **107**, 186407 (2011).

[17] T. Divoux, V. Grenard, and S. Manneville, Phys. Rev. Lett. **110**, 018304 (2013).

[18] L. J. Zapas, in *Deformation and Fracture of High Polymers*, edited by H. H. Kausch, J. A. Hassell, and R. I. Jaffee (Plenum, New York, 1974), pp. 381–395.

[19] S. M. Rubinstein, G. Cohen, and J. Fineberg, Phys. Rev. Lett. **96**, 256103 (2006).

[20] S. Dillavou and S. M. Rubinstein, Phys. Rev. Lett. **120**, 224101 (2018).

[21] K. Matan, R. B. Williams, T. A. Witten, and S. R. Nagel, Phys. Rev. Lett. **88**, 076101 (2002).

[22] Y. Lahini, O. Gottesman, A. Amir, and S. M. Rubinstein, Phys. Rev. Lett. **118**, 085501 (2017).

[23] J. B. Knight, C. G. Fandrich, C. N. Lau, H. M. Jaeger, and S. R. Nagel, Phys. Rev. E **51**, 3957 (1995).

[24] A. Prados and E. Trizac, Phys. Rev. Lett. **112**, 198001 (2014).

[25] C. Josserand, A. V. Tkachenko, D. M. Mueth, and H. M. Jaeger, Phys. Rev. Lett. **85**, 3632 (2000).

[26] K. A. Murphy, J. W. Kruppe, and H. M. Jaeger, Phys. Rev. Lett. **124**, 168002 (2020).

[27] G. B. McKenna, J. Phys.: Condens. Matter **15**, S737 (2003).

[28] E. Bertin, J. Bouchaud, J. Drouffe, and C. Godreche, J. Phys. A **36**, 10701 (2003).

[29] P. Sibani and G. G. Kenning, Phys. Rev. E **81**, 011108 (2010).

[30] A. Amir, Y. Oreg, and Y. Imry, Proc. Natl. Acad. Sci. USA **109**, 1850 (2012).

[31] S. Merabia and D. Long, J. Chem. Phys. **125**, 234901 (2006).

[32] D. R. Long, L. Conca, and P. Sotta, Phys. Rev. Mater. **2**, 105601 (2018).

[33] L. S. Loo, R. E. Cohen, and K. K. Gleason, Science **288**, 116 (2000).

[34] H.-N. Lee, K. Paeng, S. F. Swallen, and M. D. Ediger, J. Chem. Phys. **128**, 134902 (2008).

[35] H.-N. Lee, K. Paeng, S. F. Swallen, and M. D. Ediger, Science **323**, 231 (2009).

[36] H.-N. Lee, R. A. Riggleman, J. J. de Pablo, and M. D. Ediger, Macromolecules **42**, 4328 (2009).

[37] H.-N. Lee and M. D. Ediger, Macromolecules **43**, 5863 (2010).

[38] R. Perez-Aparicio, D. Cottinet, C. Crauste-Thibierge, L. Vanel, P. Sotta, J.-Y. Delannoy, D. R. Long, and S. Ciliberto, Macromolecules **49**, 3889 (2016).

[39] R. Sahli, J. Hem, C. Crauste-Thibierge, F. Clement, D. R. Long, and S. Ciliberto, Phys. Rev. Mater. **4**, 035601 (2020).

[40] J. Kalfus, A. Detwiler, and A. J. Lesser, Macromolecules **45**, 4839 (2012).

[41] R. S. Hoy and M. O. Robbins, Polymer Phys. **47**, 1406 (2009).

[42] K. S. Schweizer and E. J. Saltzman, J. Chem. Phys. **121**, 1984 (2004).

[43] K. Chen and K. S. Schweizer, Phys. Rev. Lett. **102**, 038301 (2009).

[44] L. Conca, A. Dequidt, P. Sotta, and D. R. Long, Macromolecules **50**, 9456 (2017).

[45] R. A. Riggleman, H.-N. Lee, M. D. Ediger, and J. J. de Pablo, Phys. Rev. Lett. **99**, 215501 (2007).

[46] Polycarbonate is a B-type dipole polymer [47,57]. In the high temperature range, we did not observe any peak at lower frequencies than the one corresponding to the α-relaxation process as is observed when A-type dipoles are present [47].

[47] F. Kremer and A. Schonhals, *Broadband Dielectric Spectroscopy* (Springer-Verlag, Berlin, 2003).

[48] R. Pérez-Aparicio, C. Crauste-Thibierge, D. Cottinet, M. Tanase, P. Metz, L. Bellon, A. Naert, and S. Ciliberto, Rev. Sci. Instrum. **86**, 044702 (2015).

[49] The sample deformation is homogeneous and there is no necking until the sample failure which occurs for $\lambda \geqslant 1.8$.

[50] Note that by measuring dielectric susceptibility, we measure so-called retardation times and not relaxation times. Relaxation times are associated to the relaxation of a modulus, e.g., a stress or an electric field, and retardation times are associated to the relaxation of a compliance, that is, a deformation in mechanical experiment or a polarization in dielectric experiments. Note that when there is only one relaxation time in the spectrum, the relation between both times is $\tau_{\text{retardation}} = \epsilon_0/\epsilon_\infty \tau_\alpha$ where ϵ_0 and ϵ_∞ are the low and high frequency dielectric susceptibility, respectively [58]. This ratio may be large for some systems [58], but for polycarbonate [38] it is about 1.12. Even if the ratio between both dominant retardation and relaxation times may be larger in the presence of a broad distribution of relaxation times [59], it is still expected to remain of order unity for our samples.

[51] S. Havriliak and S. Negami, J. Polym. Sci. Part C **14**, 99 (1966).

[52] $\tau_\alpha = [\Delta \sin(\beta\pi/2)]^{1/\beta} \tau_{\text{eff}}$ where $\Delta = (\epsilon_0 - \epsilon_\infty)/\epsilon_\infty$ is the dielectric strength. See [39] for details.

[53] C. Bauwens-Crowet and J. C. Bauwens, Polymer **23**, 1599 (1982).

[54] H. E. H. Meijer and L. E. Govaert, Prog. Polym. Sci. **30**, 915 (2005).

[55] E. T. J. Klompen, T. A. P. Engels, L. E. Govaert, and H. E. H. Meijer, Macromolecules **38**, 6997 (2005).

[56] *Polymer Glasses*, edited by C. B. Roth (CRC Press, Boca Raton, FL, 2017).

[57] G. Katana, F. Kremer, E. W. Fischer, and R. Plaetschke, Macromolecules **26**, 3075 (1993).

[58] R. Richert and H. Wagner, Solid State Ionics **105**, 167 (1998).

[59] J. Jackle and R. Richert, Phys. Rev. E **77**, 031201 (2008).